Elements of Electromagnetic Theory for GPR Applications

J. M. Carcione*, Istituto Nazionale di Oceanografia e di Geofisica Sperimentale (OGS), Trieste, Italy

M. A. B. Botelho, Universidade Federal da Bahia, Salvador, Brazil.

This paper was prepared for presentation at the 9th International Congress of The Brazilian Geophysical Society held in Salvador, Brazil, 11-14 September 2005.

Abstract

We develop some aspects of the electromagnetic theory regarding the application of the ground-penetrating radar (GPR), namely, a model for the composite dielectric constant, the amplitude variations with offset (AVO), the concept of exploding reflector and Backus averaging to obtain the properties of finely-layered media. The electromagnetic properties are obtained by using a generalization of the Hanai-Bruggeman (HB) equation. The HB exponent (1/3 for spherical particles) is used as a fitting parameter for a sand-clay mixture saturated with water.

We obtain the Fresnel reflection coefficients for different interfaces in subsoils saturated with air, fresh water, seawater and NAPL. The curves can be used to interpret the AVO of reflection events in the radargrams. The common feature is that the TM mode (parallel polarization) has a negative anomaly and the TE mode (perpendicular polarization) has a positive anomaly. Pseudo Brewster's angles appear beyond 40 degrees for the air/NAPL and NAPL/water interfaces and at near offsets (below 40 degrees) for the water/NAPL interface. Pseudo-critical angles are present for the water/NAPL interface. Besides the reflection strength, the phase angle can be used to discriminate between low- and high-conductivity NAPL when the properties of the upper medium are known.

The simulation of a stacked radargram requires the calculation of a set of common-source experiments and application of the standard processing sequence. To reduce the computing time, a zero-offset stacked section can be obtained with a single simulation by using the exploding-reflector concept and the non-reflecting wave equation. This non-physical modification of the wave equation implies a constant impedance model to avoid multiple reflections, which are, in principle, absent from stacked sections and constitute unwanted artifacts in migration processes. The magnetic permeability is used as a free parameter to obtain a constant impedance model. The source strength is proportional to the normal-incidence reflection coefficient. The method generates normal-incidence reflections, i.e., those having identical downgoing and upgoing wave paths. Exploding-reflector experiments provide correct traveltimes of diffractions and reflections events, in contrast to the plane-wave method.

Finally, the permittivity, conductivity and wave properties of a finely-layered medium are obtained in the long-wavelength approximation.

Introduction

The flow of seawater into fresh-water aquifers, and the injection of brine into the subsurface through hydrocarbon production wells, constitutes a major problem affecting the quality of industrial and domestic water supplies. Another problem is the contamination of the subsoil with hydrocarbons. Contaminants may exist in the gas phase, in the aqueous phase, and/or as a separate, immiscible liquid phase (i.e, Non-Aqueous Phase Liquids (NAPL)). Light NAPL (LNAPL) consist of a solution of organic compounds (e.g., petroleum hydrocarbons) which is less dense than water and forms a layer that floats on the surface of the groundwater table. On the other hand, Dense NAPL (DNAPL) consist of a solution of organic compounds (e.g., chlorinated hydrocarbons) denser than water. DNAPLs sink to the bottom of the aquifer.

GPR and electric methods have been applied with success to locate the fresh water/seawater interface in the subsoil and map the location of NAPL spills on the basis of the dielectric and electric properties. In fact, at radar frequencies, NAPL have, in general, lower permittivity and conductivity than groundwater. However, significant changes in the electrical properties of hydrocarbon spills can occur as a result of bacterial bio-degradation. In this case, the hydrocarbon spill (NAPL-2) becomes highly conductive. The electromagnetic properties of soils are modeled with the Hanai-Bruggeman formula. We assume an arbitrary pore and grain geometries (the exponent of the HB equation is used as a fitting parameter).

There are several factors determining the GPR response, namely, the transmitter-receiver configuration, the survey direction, the reflection coefficient and orientation of the target, the properties of the overlying layers, etc. The presence of seawater and the NAPL saturation can be estimated by analyzing the AVO trend of the reflection event. To study this behavior, we calculate the generalized Fresnel reflection coefficients for different cases. In particular, it is important to analyze the Brewster angle, which is observed in the TM reflection coefficient, and the type of AVO anomaly. Brewster's angles do not occur in the subsoil, since the constituent media are not perfect dielectrics, i.e., the media are lossy. However, we may consider a minimum in the absolute value of the reflection coefficient as a pseudo Brewster's angle, which can also be useful to characterize the media. The same argument can be applied to critical angles, because they are rare exceptions in lossy media. The term pseudo-critical angle is applied in this case.

There are two efficient ways, which avoid calculation of common-shot records, to simulate a zero-offset synthetic survey: the plane-wave method and the exploding-reflector method. Both approaches involve a single calculation with a time-domain modeling algorithm. The first consists in sending a horizontal localized plane-wave front down from the surface and recording the response of the subsurface model back at the surface. The travel times obtained with this method are not those obtained with the standard processing sequence. We use the exploding-reflector concept, which requires, in the first place, to halve the phase velocity. In the seismic case, the density is used as a free parameter to obtain a constant impedance model and avoid multiple reflections. From the analogy between acoustic and electromagnetic waves, the density is mathematically analogous to the magnetic permeability. We scale this property by a factor depending on the permittivity, to obtain a model where all the media have the same electromagnetic impedance.

The HB model. Permittivity and conductivity

The complex HB permittivity for two constituents satisfies the following equation:

$$\phi_2 = \left(\frac{\epsilon_1 - \epsilon^*}{\epsilon_1 - \epsilon_2}\right)\left(\frac{\epsilon_2}{\epsilon^*}\right)^W,$$

(Hanai-Bruggeman generalized)
ϵ^* = permittivity of the composite
ϕ_2: proportion of material 2 ($\phi_1 = 1 - \phi_2$)

A water-wet rock that remains percolating for small values of the porosity can be obtained from the assumption that water is the starting host material into which infinitesimal amounts of spheres of matrix and fluids are gradually included. This model is in agreement with Archie's law, i.e., it preserves the continuity of the water phase. The solution is given by W = 1/3 for spherical inclusions. When W differs from 1/3, the equation describes a porous medium of arbitrary grain shape.

To obtain the HB exponent W we fit the permittivity and conductivity of a sand/clay mixture saturated with water. The figures show the dielectric constant and conductivity for W = 0.61 (a) and W = 1/3 (b) (stars), where 0.61 is the best fit to the experimental data (diamonds with errors bars). The fact that W is equal to 0.61 indicates a significant departure of the grain shape from a sphere.

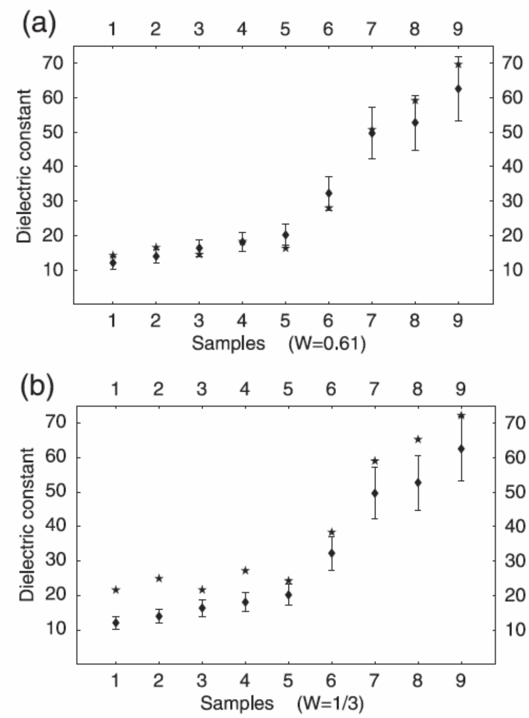

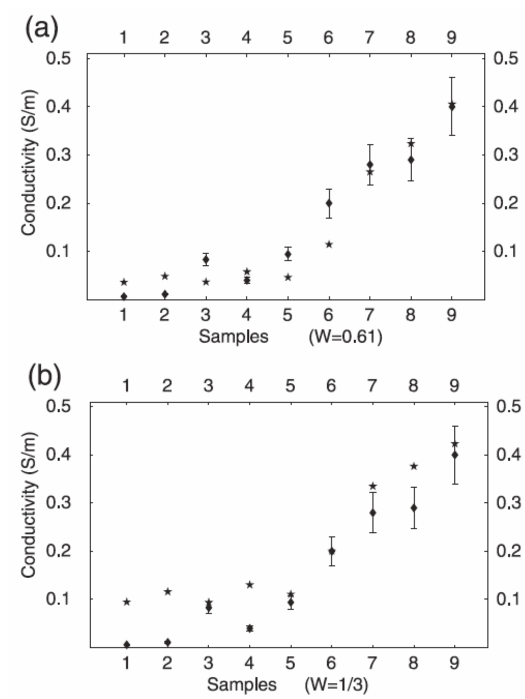

We use the HB equation twice to obtain the complex dielectric permittivity of the sediment. The mixing order is the following: sand/clay (solid) and solid/fluid.

AVO theory

The subsoil is composed of a mixture of sand, silt and clay, air, water and contaminant. The figure below shows the reflection-refraction problem and corresponding top view of the GPR antenna configurations (diagrams at the right side). (a) Parallel endfire (TM mode, parallel polarization). (b) Perpendicular broadside (TE mode, perpendicular polarization).

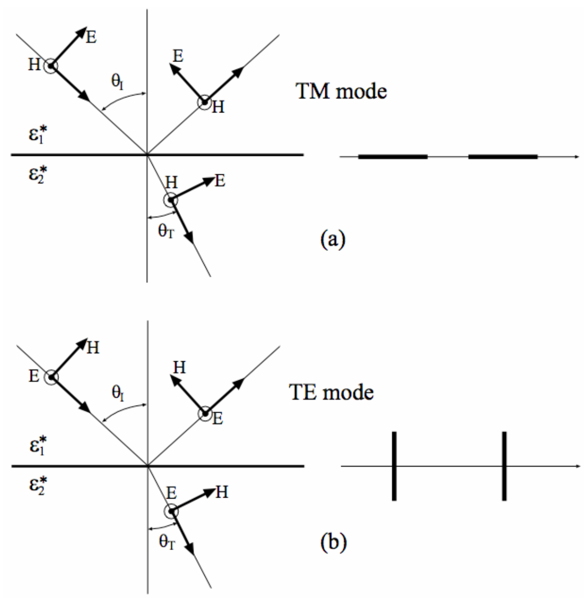

The following are the reflection and transmission coefficients, the refraction index, Snell's law for lossy media and the Brewster angle for lossless media.

$$R_{\mathrm{TM(TE)}} = \frac{n_{2(1)}\cos\theta_I - n_{1(2)}\cos\theta_T}{n_{2(1)}\cos\theta_I + n_{1(2)}\cos\theta_T}$$

$$\text{(Fresnel eqs.)}$$

$$n^2 = \frac{\epsilon^*}{\epsilon_0}, \quad \epsilon_0 = 8.85\ 10^{-12}\mathrm{F/m}$$

$$\frac{n_1}{\sin\theta_T} = \frac{n_2}{\sin\theta_I} \ \text{(Snell's law)}$$

$$\sin\theta_C = \tan\theta_B = \sqrt{\frac{\epsilon_2}{\epsilon_1}} \ \text{(Critical and Brewster angles)}$$

The interfaces considered in this work are shown in the diagram, where (a) corresponds to the case of terrestrial fresh water interacting with seawater in coastal aquifers and (b) to a floating hydrocarbon spill. The figure below the diagram shows the TM (a) and (TE) (b) Fresnel coefficients versus incidence angle for the air/water interface (model 1) and air/seawater interface (model 2). The pseudo Brewster angle occurs at nearly 70 degrees for the TM case. Beyond this angle the reflection coefficient becomes negative. The AVO anomaly is negative for the TM case and positive for the TE case, i.e., the reflection coefficients decrease and increase with increasing angle, respectively. The magnitude of the reflection coefficient is higher for seawater (model 2).

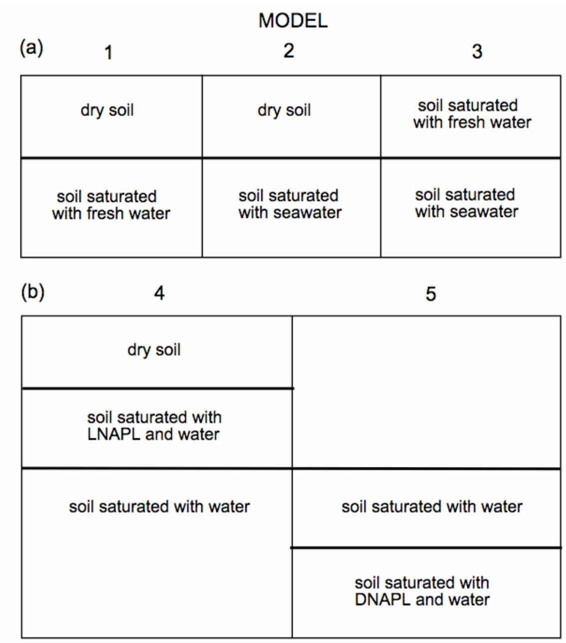

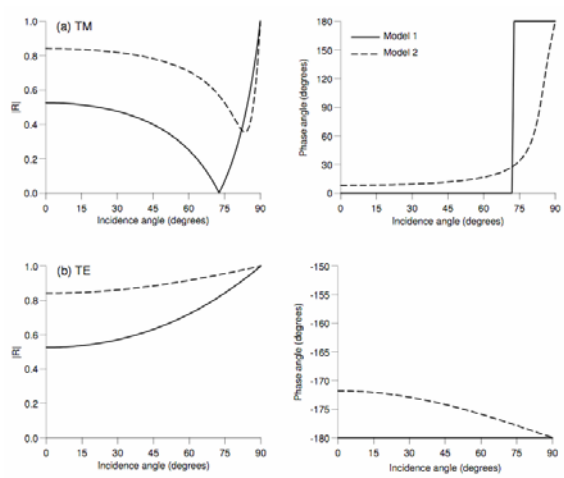

Next, we consider the water/DNAPL interface (model 5). The results for the TM coefficient are shown in the following figure for various NAPL saturations. In this case, pseudo Brewster's angles can be found at relatively near offsets, but they are more difficult to detect than those corresponding to the air/NAPL interface (not shown), since the reflection event is affected by the presence of the upper interfaces. A pseudo-critical angle occurs after the pseudo Brewster angle. The difference between the NAPL-1 and NAPL-2 (bio-degraded) cases is significant after the pseudo-critical angle. Other calculations show that the saturation can be determined on the basis of the reflection strength only for low conductivity LNAPL. The higher permittivity and conductivity for bio-degraded LNAPL causes a strong reflectivitty of the top of the hydrocarbon plume and significant energy losses through the plume. This explains the characteristic response observed in radargrams of old (bio-degraded) hydrocarbon spills (see last reference).

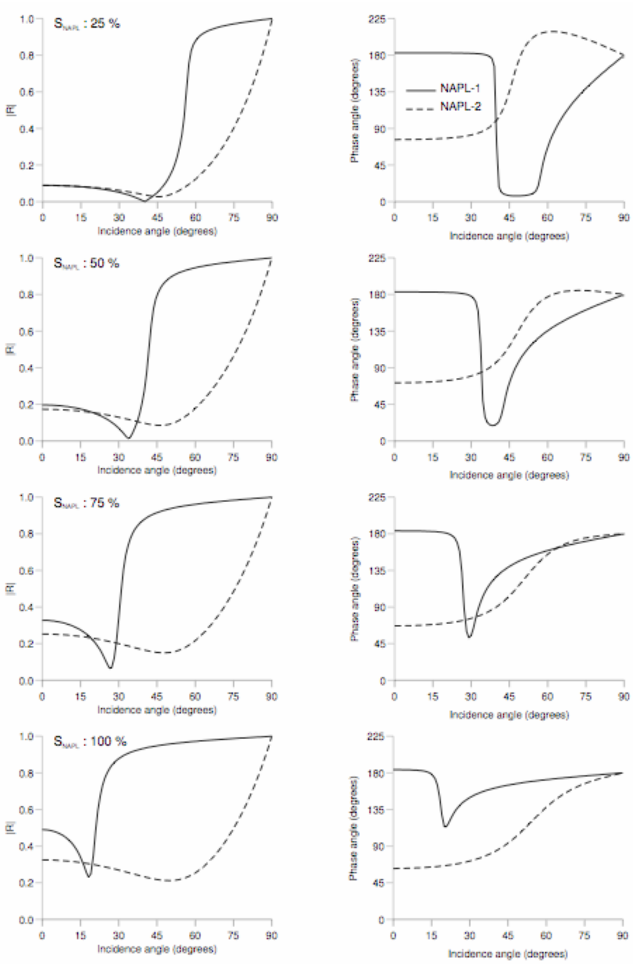

Exploding-reflector experiment

The implementation of the exploding-reflector method in GPR modeling requires:

1. A source is placed at every point on the subsurface interface.
2. The phase velocity of each medium is halved, to obtain the correct two-way travel time and amplitude decay for every diffraction and reflection event.
3. The source strength is proportional to the normal-incidence reflection coefficient at each point on the interface (a zero-offset raypath is normal to the reflecting interface).
4. To avoid multiples, we require that the electromagnetic impedance be the same for all media. Since the impedance depends on frequency, we require that the optical impedance be the same.

The recipe is:

$$\mu_0 \rightarrow 4\mu_0.$$

$$v = \frac{1}{\sqrt{\mu_0 \epsilon^*}} \rightarrow \frac{v}{2} \text{ (complex velocity)}$$

$$v_p = \left[\mathrm{Re}\left(\frac{1}{v}\right)\right]^{-1} \rightarrow \frac{v_p}{2} \text{ (phase velocity).}$$

$$\alpha = -\omega \mathrm{Im}\left(\frac{1}{v}\right) \rightarrow 2\alpha \text{ (attenuation)}$$

$$\mu \rightarrow \mu_0/a, \quad a = \sqrt{\epsilon_0/\epsilon}$$

$$\epsilon^* = \epsilon - \frac{i}{\omega}\sigma \rightarrow a\epsilon^*$$

Electromagnetic impedance:

$$I(\omega = \infty) = \sqrt{\frac{\mu}{\epsilon^*}} = \sqrt{\frac{\mu_0}{\epsilon_0}} \quad \text{for all the media}$$

Let us consider the model shown in the following figure.

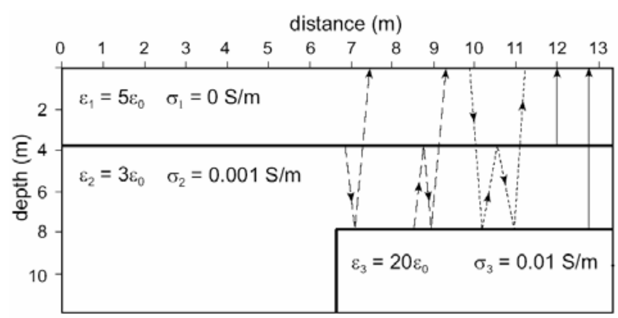

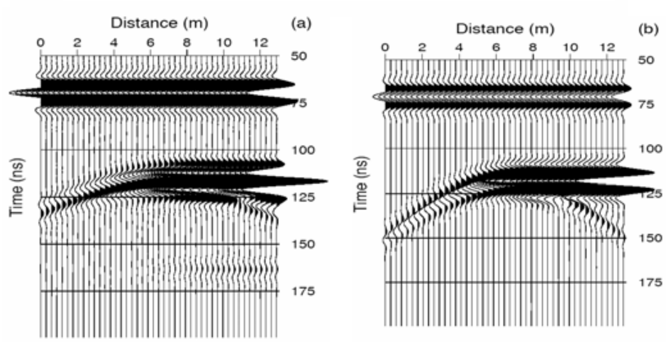

The raypaths represented with solid lines are the direct arrivals. The other events should be avoided. The dotted line is a multiple, present in the plane-wave response at 162 ns (left). The exploding-reflector traveltimes (right) are greater than the plane-wave traveltimes, and there is a change of polarity in the plane-wave response of the step.

Backus averging for electromagnetic media

The electromagnetic properties of finely plane-layered media can be obtained by the Backus averaging approach used to upscale sonic logs. Let us consider a plane-layered medium, where each layer is homogeneous, isotropic and thin compared to the wavelength of the electromagnetic wave. If the layer interfaces are parallel to the (*x*,*z*)-plane, the properties are independent of *x* and *y* and may vary with *z*. An important approximation in this context is

$$\langle fg \rangle = f \langle g \rangle,$$

where *f* is nearly constant over the averaging distance *d* and *g* may have an arbitrary dependence as a function of *z*. We express the rapidly varying fields in terms of the slowly varying fields (these are continuous across the interfaces). Then, we average by using the preceding property.

$$\mathbf{D} = \epsilon \mathbf{E} \quad \text{(constitutive equations)}$$

Continuity of $D_3, \ E_1, \ E_2$

$$D_1 = \epsilon E_1, \ D_2 = \epsilon E_2, \ E_3 = \epsilon^{-1} D_3$$

Averaging

$$\langle D_1 \rangle = \langle \epsilon \rangle \langle E_1 \rangle, \ \langle D_2 \rangle = \langle \epsilon \rangle \langle E_2 \rangle, \ \langle E_3 \rangle = \langle \epsilon^{-1} \rangle \langle D_3 \rangle$$

$$\epsilon_{11} = \epsilon_T = \langle \epsilon \rangle, \quad \epsilon_{33} = \epsilon_N = \langle \epsilon^{-1} \rangle^{-1}$$

The averaged (equivalent) medium is transversely isotropic. The averaging equations are also valid for complex permittivity. Hence the method allows us to obtain the average permittivity and conductivity.

The wave propagation theory is given for the ordinary and extraordinary waves (Carcione and Seriani, 2000).

Complex velocity of ordinary and extraordinary waves

$$v = v_o = \frac{1}{\sqrt{\mu \epsilon_T}}, \quad v = v_e = \sqrt{\frac{l_1^2 + l_2^2}{\mu \epsilon_N} + \frac{l_3^2}{\mu \epsilon_T}}$$

l_i: direction cosines

Phase velocity, attenuation and quality factor

$$v_p = \left[\mathrm{Re}\left(\frac{1}{v} \right) \right]^{-1}, \quad \alpha = -\omega \mathrm{Im}\left(\frac{1}{v} \right), \quad Q = \frac{\mathrm{Re}(v^2)}{\mathrm{Im}(v^2)}$$

Energy velocity (wavefront) of the extraordinary TM wave in the (1,3)-plane

$$\mathbf{v}_E^{\mathrm{TM}} = \frac{v_{pe}}{\mu \mathrm{Re}(v_e)} \left[\mathrm{Re}\left(\frac{l_1}{\epsilon_N v_e} \right) \hat{\mathbf{e}}_1 + \mathrm{Re}\left(\frac{l_3}{\epsilon_T v_e} \right) \hat{\mathbf{e}}_3 \right].$$

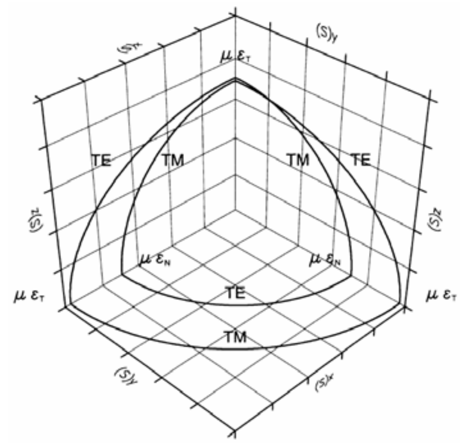

The figure shows the intersection of the slowness surface with the principal planes. The corresponding waves are either transverse electric (TE) or transverse magnetic (TM). The values on the axes refer to the square of the complex slowness.

References

Baradello, L., Carcione, J. M., and Gei, D., 2004, Fast monostatic GPR modeling, Geophysics, **69**, 466-471.

Carcione, J. M., Botelho, M. A. B., Osella, A., and de la Vega, M., 2004, Fresnel reflection coefficients for GPR-AVO analysis and detection of seawater and NAPL contaminants, Near Surface Geophysics, submitted.

Carcione, J. M., and Robinson, E., 2002, On the acoustic-electromagnetic analogy for the reflection-refraction problem, Studia Geoph. et Geod., **46**, 321-345.

Carcione, J. M., and Seriani, G., 2000, An electromagnetic modelling tool for the detection of hydrocarbons in the subsoil, Geophys. Prosp., **48**, 231-256.

Carcione, J. M., Seriani, G., and Gei, D., 2003, Acoustic and electromagnetic properties of soils saturated with salt water and NAPL, J. Appl. Geophys., **52**, 177-191.